#3668

CHALMERS UNIVERSITY OF TECHNOLOGY
Division of Structural Design
1986:5
ISSN 0281-1863

FREQUENCY RESPONSE FUNCTIONS FOR DIFFERENTIAL PRESSURE MEASUREMENT TUBING

by

Jan Gustén and Bengt Magnusson

1986

ABSTRACT

Transfer functions for differential pressure measurement tubing are determined in the laboratory for tube lengths 25, 50 and 115 m. Effects of the location of the transducer in the measuring system are examined. The transfer function obtained for the tube length 115 m is compared to results obtained in a full-scale experiment.

Key words

Wind pressure, differential pressure measurement, transfer function

PREFACE

This report has been worked out at the Division of Structural Design, Chalmers University of Technology, under the supervision of Dr K. Handa. Financial support has been obtained from the Swedish Council for Building Research, and the Swedish Contractors' Research and Development Foundation.

The authors gratefully acknowledge the valuable comments of Dr K. Handa, and much practical help from Mr H. Bäckberg.

Thanks are also directed to Mrs M. Micrander for her typewriting and to Mr M. Svoboda for his figures.

Göteborg in December

Jan Gustén
Bengt Magnusson

C O N T E N T S

NOTATION

$C_{xy}(f)$	Real part of cross spectrum
$G_{xx}(f)$, $G_{yy}(f)$	One-sided power spectrum
$G_{xy}(f)$	One-sided cross spectrum
$H(f)$	Transfer function
$Q_{xy}(f)$	Imaginary part of cross spectrum
a_o	velocity of sound in air
f	frequency
ℓ	length
n	order number
$\Theta_{xy}(f)$	phase shift
$\gamma^2(f)$	coherence function
ω	angular frequency
ρ_{xy}	correlation coefficient in frequency domain

1 INTRODUCTION

Pressure differences caused by wind or temperature are commonly measured by pressure transducers, or some times by liquid manometers. On practical grounds, the measurement device cannot always be located immediately adjacent to the surface of a wall where the pressure is to be determined. Thus, some kind of tubing must transfer the pressure at point X to a differential pressure transducer, located at Y , see Figure 1.1. The pressure transducer should also be connected to a reference pressure at location Z since absolute pressure fluctuations cannot be measured. The measurement system is characterized by the dimensions of the tubes and the internal volume of the transducer.

When a fluctuating pressure is applied at the measuring point X , a distorted pressure difference is registered at Y due to damping and resonances in the tubing.

Previous research on the effects of tubing on the measurement of fluctuating pressures has mainly been directed towards applications in wind tunnel engineering, see for instance Bergh and Tijdeman (1965), and Irwin et al. (1979).

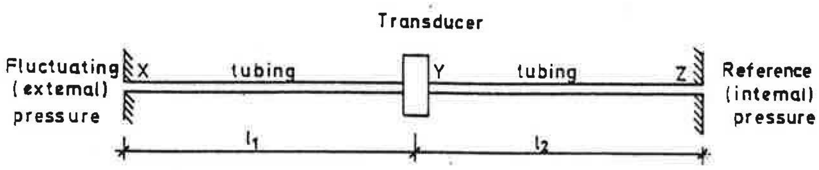

Figure 1.1 System for measurement of differential pressures

In order to employ the measurement system illustrated in Figure 1.1 for full-scale investigations, the frequency response characteristics must be determined. In the following, three different lengths of tubing are studied: 25, 50 and 115 m. The tubing has in all cases an internal diameter of 5 mm, and an external diameter of 8 mm, and it is manufactured from polyethene.

2 DETERMINATION OF TRANSFER FUNCTIONS

2.1 Theoretical considerations

The system is assumed to be linear, which, as soon as the frequency domain representation (power spectrum) $G_{yy}(f)$ of the signal at point Y is found, enables the calculation of the power spectrum $G_{xx}(f)$ at point X which is the quantity of interest. The input power spectrum $G_{xx}(f)$ is determined from the relationship

$$G_{yy}(f) = |H(f)|^2 G_{xx}(f) \tag{2.1}$$

where H(f) is the transfer function of the system. Thus, in a field measurement situation, the transfer function H(f) must be known.

The most convenient way of determining the transfer function H(f) is to use the relationship

$$G_{xy}(f) = H(f) \cdot G_{xx}(f) \tag{2.2}$$

where $G_{xy}(f)$ is the cross spectrum between input at X and output at Y. Consequently the complex transfer function is given by

$$H(f) = \frac{G_{xy}(f)}{G_{xx}(f)} \tag{2.3}$$

where $G_{xx}(f)$ and $G_{xy}(f)$ are determined from results obtained in the laboratory.

The phase shift $\theta_{xy}(f)$ between input at X and output at Y can be obtained from

$$\theta_{xy}(f) = \operatorname{arctg}\left[\frac{Q_{xy}(f)}{C_{xy}(f)}\right] \qquad (2.4)$$

where $C_{xy}(f)$ is the real (coincident) part of the cross spectrum, and $Q_{xy}(f)$ is the imaginary (quadrature) part.

The coherence function $\gamma_{xy}(f)$ defined by

$$\gamma^2_{xy}(f) = \frac{|G_{xy}(f)|^2}{G_{xx}(f)G_{yy}(f)} \qquad (2.5)$$

gives information about the extent to which the output at Y is explained by the input at X , cf. Bendat and Piersol (1971). For a perfectly linear system with no extraneous noise present, the coherence coefficient should equal unity.

2.2 Experimental procedures

The experimental set-up is illustrated in Figure 2.1. The tubing is connected to an air-tight box which has a membrane. The membrane can be excited by applying an electrical signal. The differential pressure is measured at X and Y by Validyne MP45 transducers with measurement range ±200 Pa. The measured signals are recorded on a tape recorder, TEAC R-71, and subsequently sampled by an A/D-converter on a Digital MINC. Thereafter the data are transferred to the IBM 3081 computer at Gothenburg Universities' Computing Centre, where spectral quantities and transfer functions are evaluated by the computer program DACSA, Handa (1985).

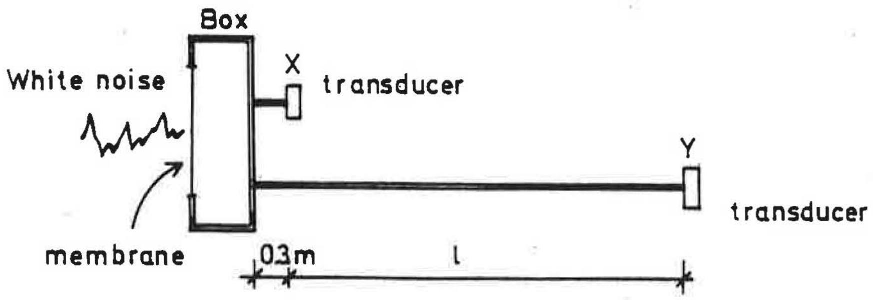

Figure 2.1 Experimental set-up for determination of the transfer function of the tubing. First series of experiments with straight tubing.
Length ℓ = 25, 50 and 115 m.

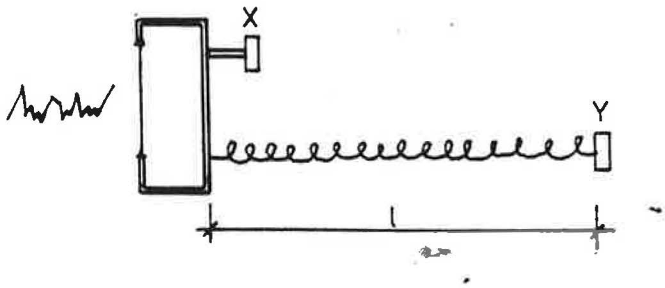

Figure 2.2 Experimental set-up for determination of the transfer function of rolled rubing.
Length ℓ = 25, 50 and 115 m.

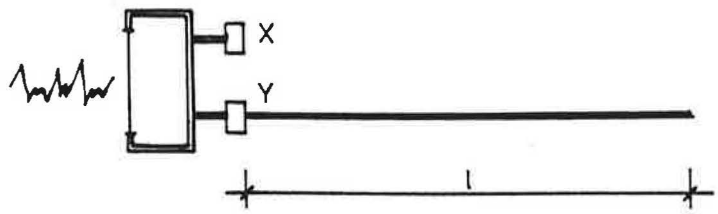

Figure 2.3 Experimental set-up for determination of the effect of (straight) tubing on the reference pressure.
Length ℓ = 25, 50 and 115 m.

Three series of experiments were conducted, the first one as illustrated in Figure 2.1.

The second series of experiments is identical, with the exception that the tubing was not straight, but rolled in bundles with about 0.7 m diameter, see Figure 2.2.

The final series of experiments were conducted in order to determine the influence of the location of the transducer within the measurement system. Different lengths of the tubing on the reference pressure side were studied, see Figure 2.3.

In all the experiments, a white noise signal in the range 0-20 Hz was applied to the membrane, see Figure 2.4, which gave a zero mean differential pressure over the transducers and peak values of the order 20 Pa. All signals were sampled with a sampling rate of 50 Hz, and the spectral quantities were calculated on the basis of 1024 data points and smoothed by taking average values over 31 spectra, cf. Handa (1985).

2.3 Transfer functions for straight tubing

The transfer functions determined according to Eq. (2.3) are illustrated in Figure 2.5, while the corresponding coherence functions and phase shifts are shown in Figures 2.6 and 2.7, respectively.

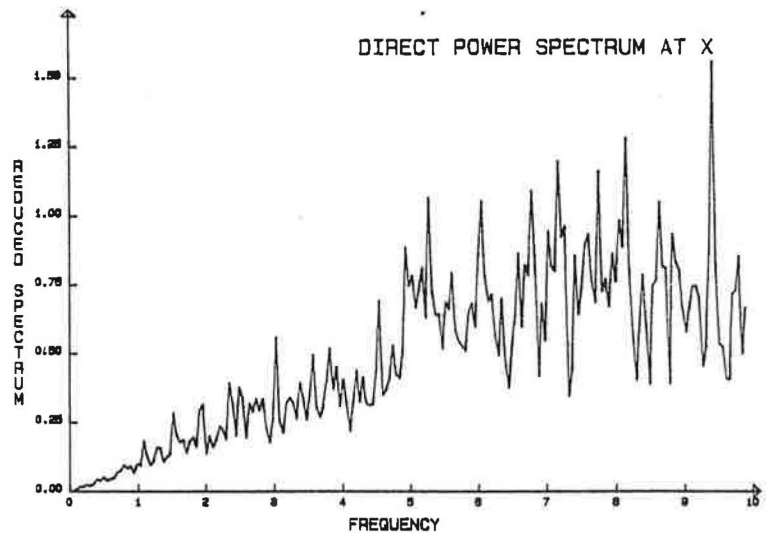

Figure 2.4 Reduced power spectrum for differential pressure at X for a white noise signal.

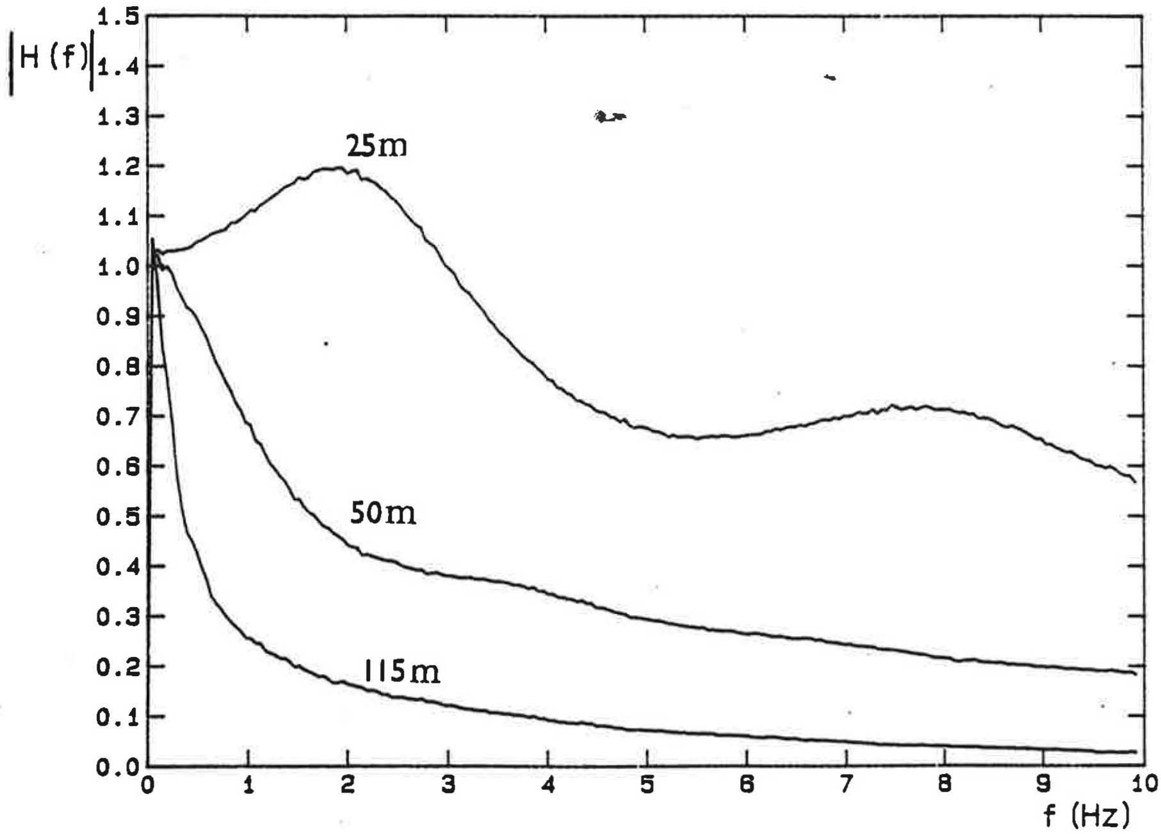

Figure 2.5 Absolute magnitude of the transfer functions for straight tubing with ℓ = 25, 50 and 115 m.

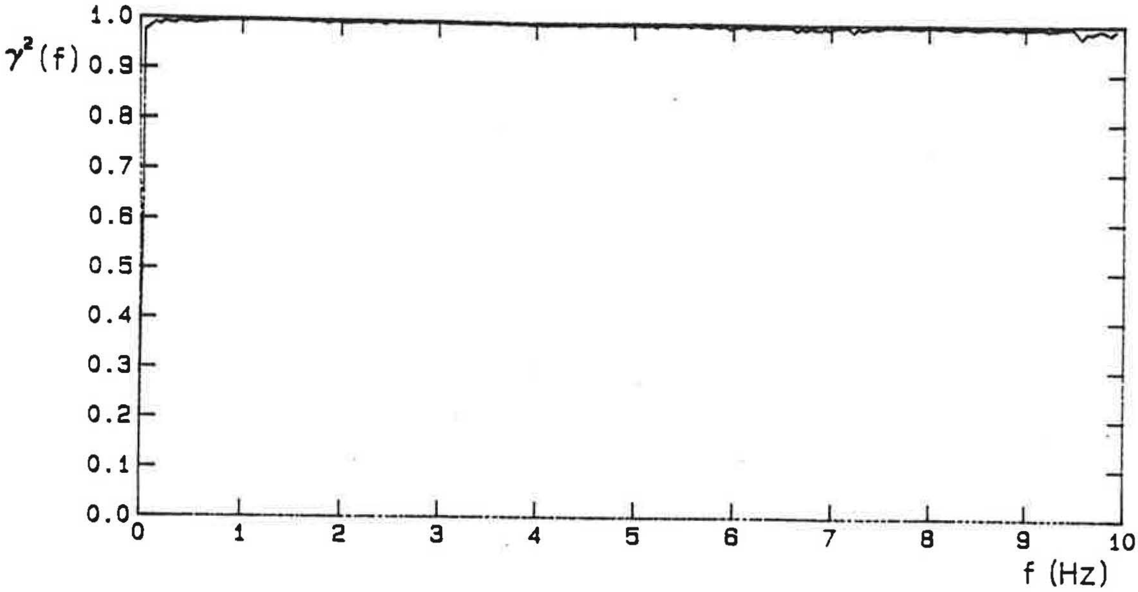

Figure 2.6 Coherence functions for straight tubing. The curves for the different lengths coincide.

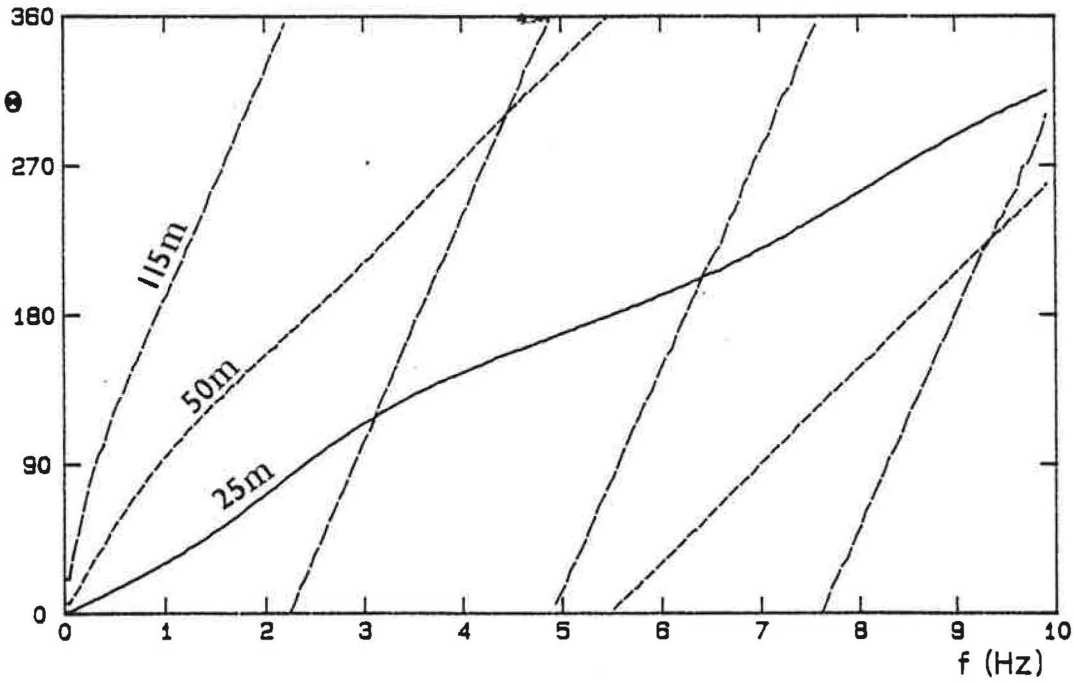

Figure 2.7 Phase shift in degrees for straight tubing.

An ocular inspection of the transfer function obtained for tube length 115 m, shows that at the frequency range of interest, below 1 Hz, the function exhibits a very steep gradient. Therefore, it was decided to carry out a further investigation of this tube length in the low frequency range. For that purpose, a low frequency random signal generator was employed and the sampling frequency was chosen to be 10 Hz since the analog low-pass filters at hand were fixed at 5 Hz.

The analysis was based upon the computer program FFTZ, Magnusson (1986). The results obtained are shown in Figures 2.8 - 2.10.

From Figure 2.8 it is readily noticed that for frequencies below 0.07 Hz the pressure fluctuations are transferred through the tubing without distortion.

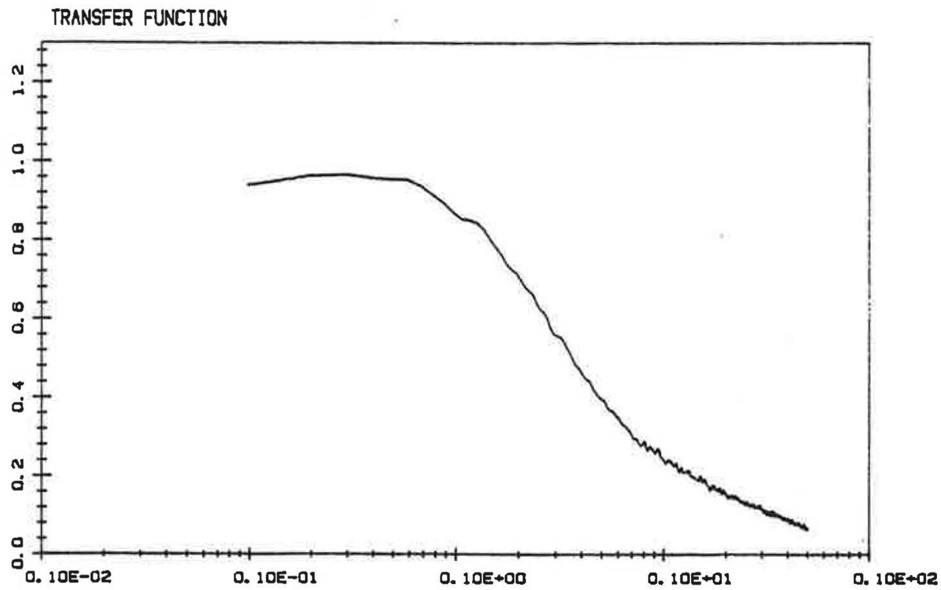

Figure 2.8 Transfer function for 115 m tubing. Logarithmic abscissae.

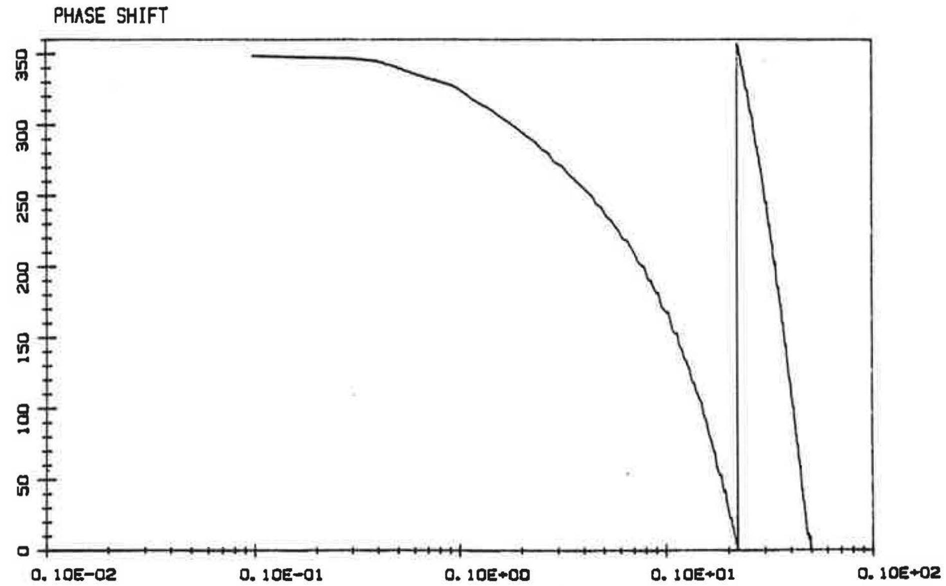

Figure 2.9   Phase shift for 115 m tubing

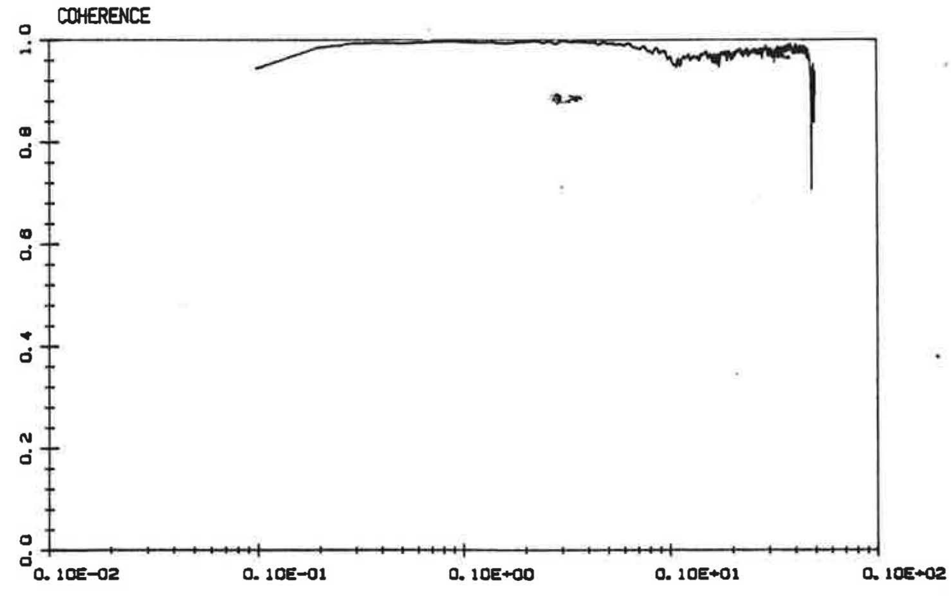

Figure 2.10   Coherence function for 115 m tubing

2.4 Transfer functions for rolled tubing

The experimental set-up according to Figure 2.2 gives results as shown in Figures 2.11 - 2.13.

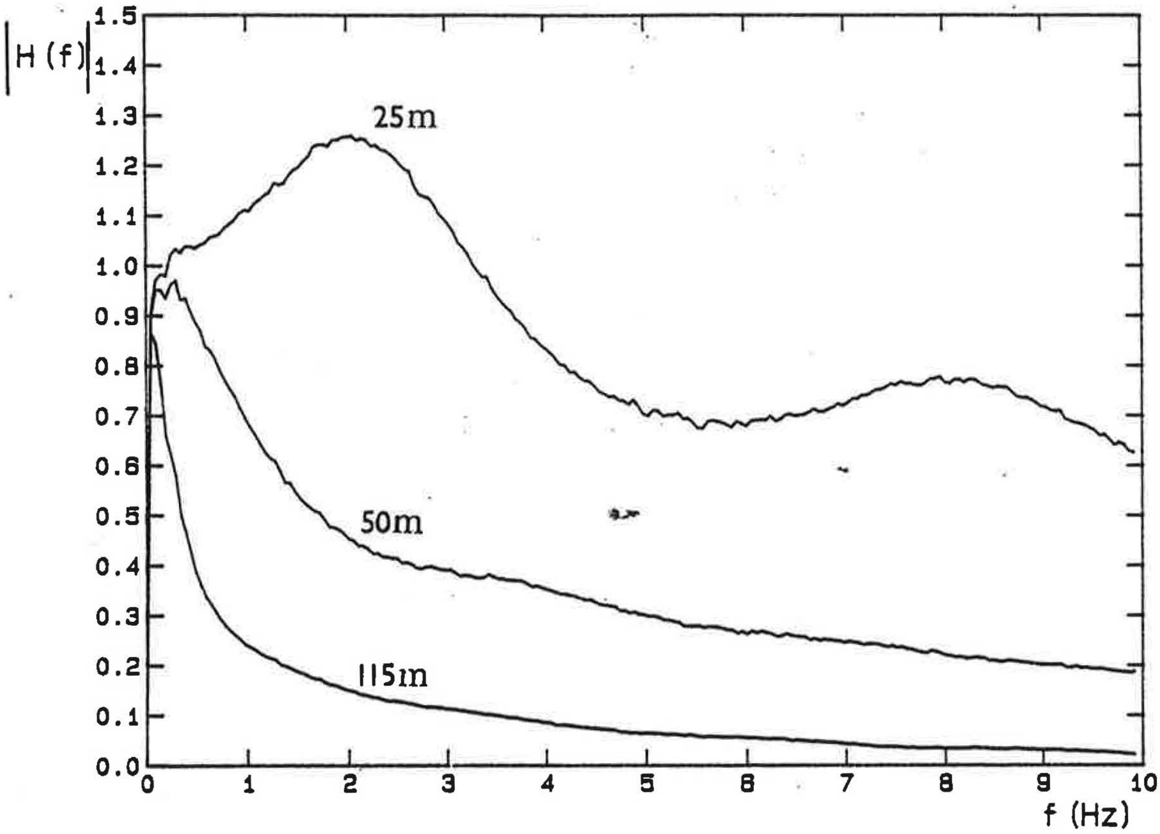

Figure 2.11 Absolute magnitude of the transfer functions for rolled tubing with ℓ = 25, 50 and 115 m.

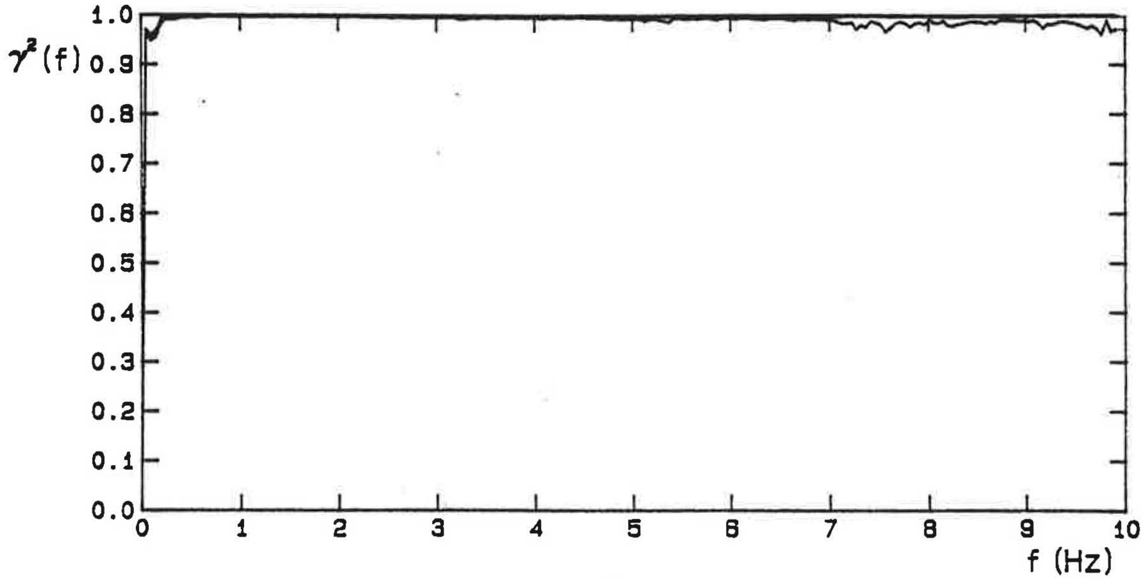

Figure 2.12 Coherence functions for rolled tubing

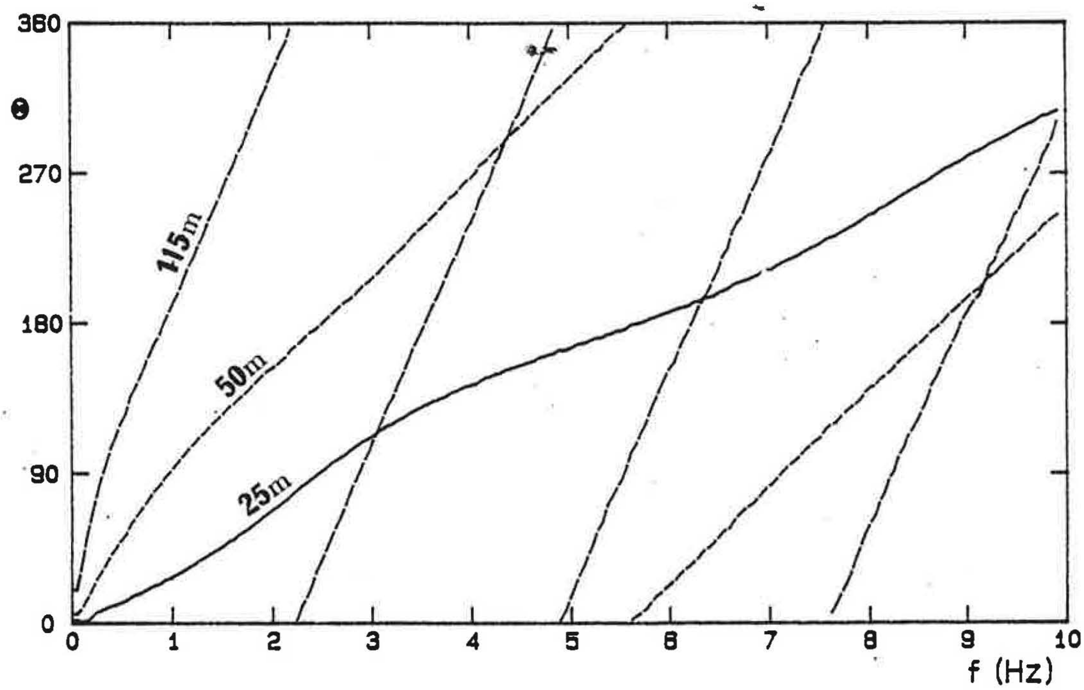

Figure 2.13 Phase shift for rolled tubing

2.5 Effects of tubing on reference pressure

Figure 2.14 shows the transfer function determined according to the experimental set-up illustrated in Figure 2.3.

The case where the magnitude of the transfer function $|H(f)|$ is fairly constant and close to 1.0 all over the frequency range corresponds to the set-up shown in Figure 2.3, while the resonant and damped function corresponds to Figure 2.1. Similar results are obtained for the other lengths of tubing.

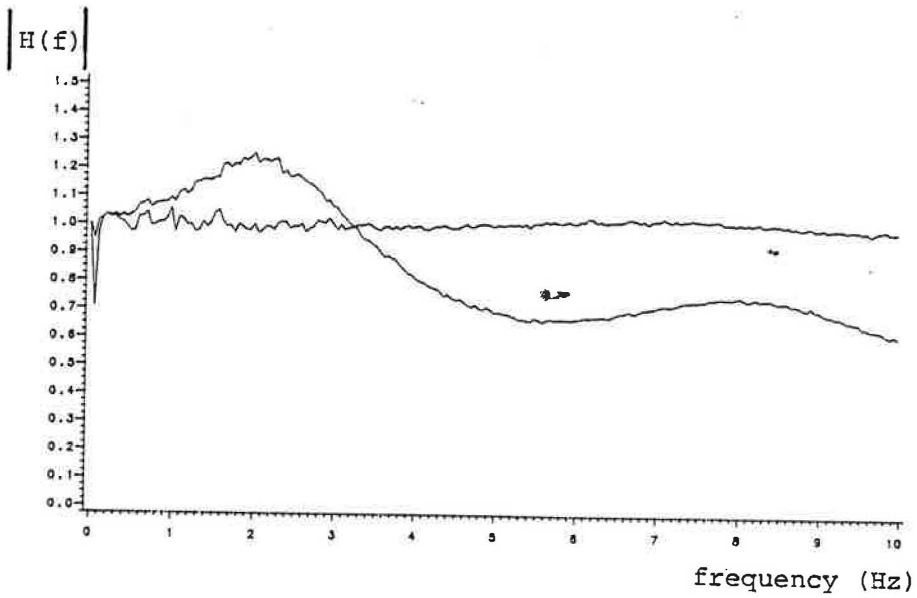

Figure 2.14 Transfer functions for different locations of the transducer. Tube length 25 m.

3 DISCUSSION AND CONCLUSIONS

3.1 General

From the laboratory experiments, absolute magnitudes of transfer functions $|H(f)|$ have been determined for three different lengths of tubing: 25, 50 and 115 m. For tube length 25 m, pronounced eigenfrequencies are obtained, whilst the two longer tubes exhibit very weak resonances. The damping in the system increases with the tube length and as a consequence the reliability of the data decreases considerably due to extraneous noise caused by the measurement system. This effect can only partly be accounted for by employing low-pass filters. From that point of view, it is obviously better to employ a measurement system where the transducers are placed immediately adjacent to measurement point, and hence to place the tubing on the reference pressure side.

The resonance frequencies of a tube with length ℓ are given by the solution of the equation

$$\frac{\omega \ell}{a_o} = n \frac{\pi}{2} \quad ; \quad n = 1, 3, 5, \ldots \tag{3.1}$$

where a_o is the propagation velocity of sound waves in air, and $\omega = 2\pi f$.

Eq. (3.1) yields the following resonance frequencies

25 m : $f = n \cdot 3.4$ Hz
50 m : $f = n \cdot 1.7$ Hz
115 m : $f = n \cdot 0.74$ Hz

Inspection of the transfer functions obtained see Sections 2.3 and 2.4, shows that the resonance frequencies are lower than predicted by Eq.(3.1). This fact is attributed to the heavy damping in the system.

As mentioned, several effects have influence on the results obtained. Besides the performance of the transducers and the amplifiers, as well as the shape of inlet and outlet of the tubing, the shape of the tubing (rolled or straight) is shown to have influence on the transfer function.

The study presented has not considered temperature effects, since all experiments were conducted in a laboratory environment at +20°C. According to Bergh & Tijdeman (1965), temperature has a minor influence on the transfer function.

Further, no attention has been paid to the possible influence of the mean and differential pressure level (peak-value or RMS-value). The mentioned reference shows a considerable influence of the mean pressure level on the resulting transfer function. However, the pressure level studied in a full-scale environment is of the order 100 Pa while the mean pressure levels studied by Berg and Tijdeman were of the order 100 kPa. Therefore, it seems to be reasonable to conclude that the results of the investigation can be employed for practical measurement purposes. However, as will be shown below, due regard must be paid to the possible influence of spurious noise, especially for the 115 m tubing. The resolution capacity of the A/D-converter also puts limitations on the employment of transfer functions with small magnitudes.

3.2 Applications in practical measurement situations

Consider a measurement situation as in Figure 3.1. The pressures at X are measured by means of transducers located at Y . Spectral estimates at location Y can be obtained directly by means of an FFT-analysis of signals recorded. Thus, at location Y the quantities $G_{y_1y_1}(f)$, $G_{y_2y_2}(f)$ and $G_{y_1y_2}(f)$ are easily determined. However, these quantities are of minor interest, rather the corresponding quantities at location X are of concern.

On the assumption that both the tubes have the same transfer function H(f) , the direct power spectral estimates at location X are determined as

$$G_{x_1x_1}(f) = \frac{1}{|H(f)|^2} G_{y_1y_1}(f) \tag{3.1a}$$

$$G_{x_2x_2}(f) = \frac{1}{|H(f)|^2} G_{y_2y_2}(f) \tag{3.1b}$$

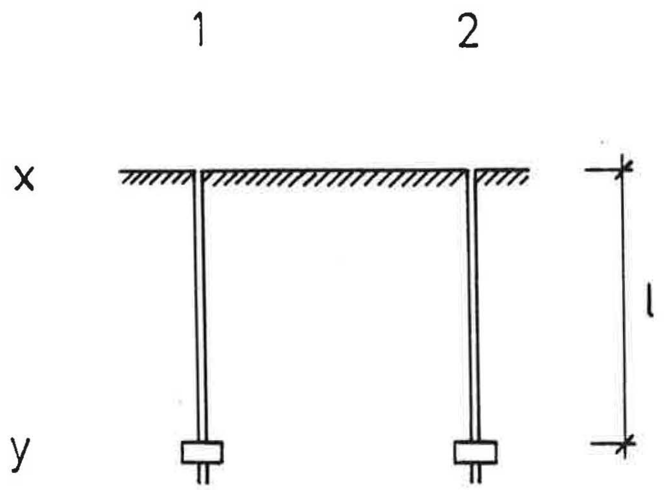

Figure 3.1 A field measurement situation

The cross-spectrum $G_{x_1x_2}(f)$ is determined by the relation, Robson (1963)[1, 2]

$$G_{y_1y_2}(f) = H^*(f)H(f)G_{x_1x_2}(f) \qquad (3.2a)$$

which yields

$$G_{x_1x_2}(f) = \frac{1}{|H(f)|^2} G_{y_1y_2}(f) \qquad (3.2b)$$

The cross-spectrum can be represented in a non-dimensionalized form by the cross-correlation coefficient

$$\rho_{x_1x_2}(f) = \frac{G_{x_1x_2}(f)}{\sqrt{G_{x_1x_1}(f)G_{x_2x_2}(f)}} \qquad (3.3)$$

which, by introduction of Eqs (3.1) and (3.2), gives

$$\rho_{x_1x_2}(f) = \rho_{y_1y_2}(f) \qquad (3.4)$$

Since

$$\gamma^2_{x_1x_2}(f) = \rho^*_{x_1x_2}(f)\rho_{x_1x_2}(f)$$

it follows immediately that

$$\gamma^2_{x_1x_2}(f) = \gamma^2_{y_1y_2}(f) \qquad (3.5)$$

As an example of the above discussion, the results from a full-scale experiment, conducted in a 100 m high chimney, Figure 3.2, are shown below.

At two different points on the circumference near the top of the chimney, the differential pressures were measured during 30 minutes. The pressures were measured with two transducers placed at the top of the chimney, and simultaneously with two transducers placed at the base of the chimney, see Figure 3.2.

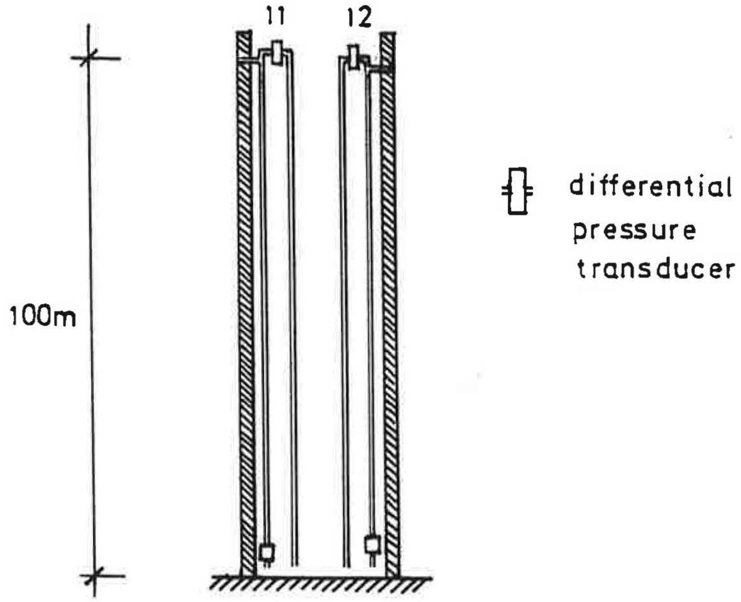

Figure 3.2 Full-scale measurement for testing the transfer function for 115 m tubing

The signals were sampled at the rate 10 Hz, after passing low-pass filters set at 5 Hz. The resultant spectra were obtained by averaging over 95 spectra, each based upon 1024 data points.

Figure 3.3 shows the transfer functions obtained. For frequencies below 1 Hz, these functions are in good agreement with the function determined in a laboratory environment. However, from the coherence functions and the phase shifts determined, Figures 3.4 - 3.5, it is obvious that the tube length 115 m cannot be employed for studies of pressure fluctuations with periods shorter than 1 sec. It is also evident that the tubes do not have identical properties. Figures 3.6 - 3.12 and Table 3.1 show some quantities of interest. In the figures, the solid line represents the quantity as measured at the top, while the dashed line represents the corresponding quantity as measured at the base and adjusted accordingly.

Table 3.1 Some spectral quantities, as measured at the top of the chimney, and as measured at the base and adjusted accordingly. The percentages given refer to the values obtained at the top.

Quantity	Tube 11			Tube 12		
	Top	Base	% Deviation	Top	Base	% Deviation
Mean pressure (Pa)	70.8	72.9	3.0	55.4	56.3	1.6
Standard deviation (Pa)	12.5	13.5	8.0	19.0	19.2	1.1
Maximum pressure[*)] (Pa)	106.7	110.6	3.7	107.5	107.2	-0.3
Correlation[**)] time (s)	2.15	2.13	-0.9	2.80	2.78	-0.7

*) Evaluated as $\bar{p} + g\sigma_p$, where $g = \sqrt{2\ln\nu T} + 0.577/\sqrt{2\ln\nu T}$

**) Evaluated as $\int_{\rho(\tau) > 0} \rho(\tau)\,d\tau$

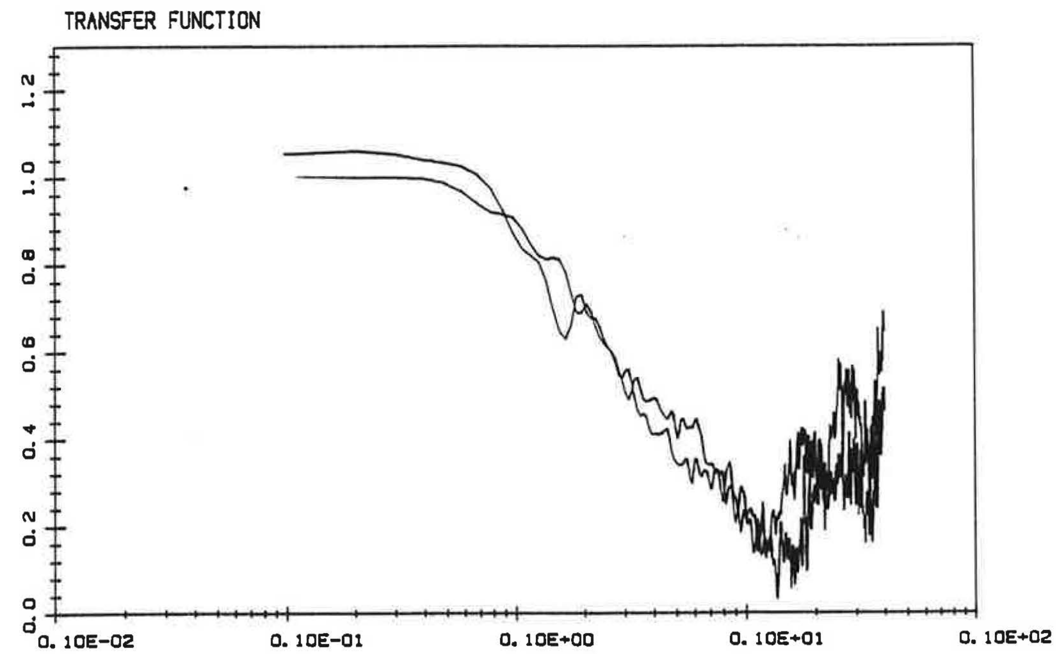

Figure 3.3 Transfer functions for 115 m tubing as determined in a full-scale experiment

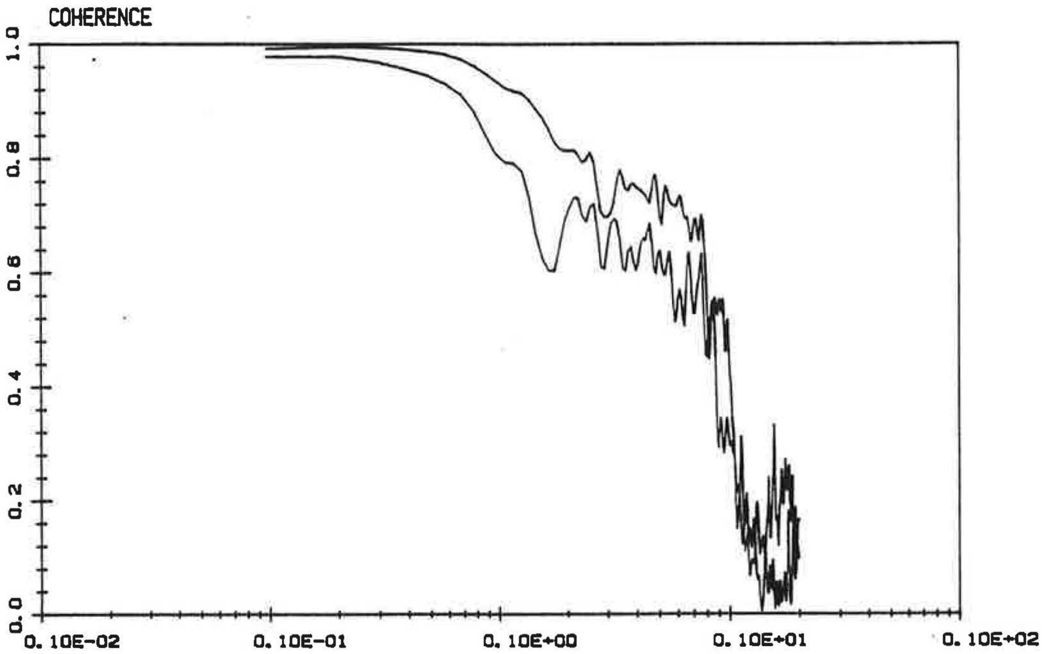

Figure 3.4 Coherence functions corresponding to the transfer functions in Figure 3.3

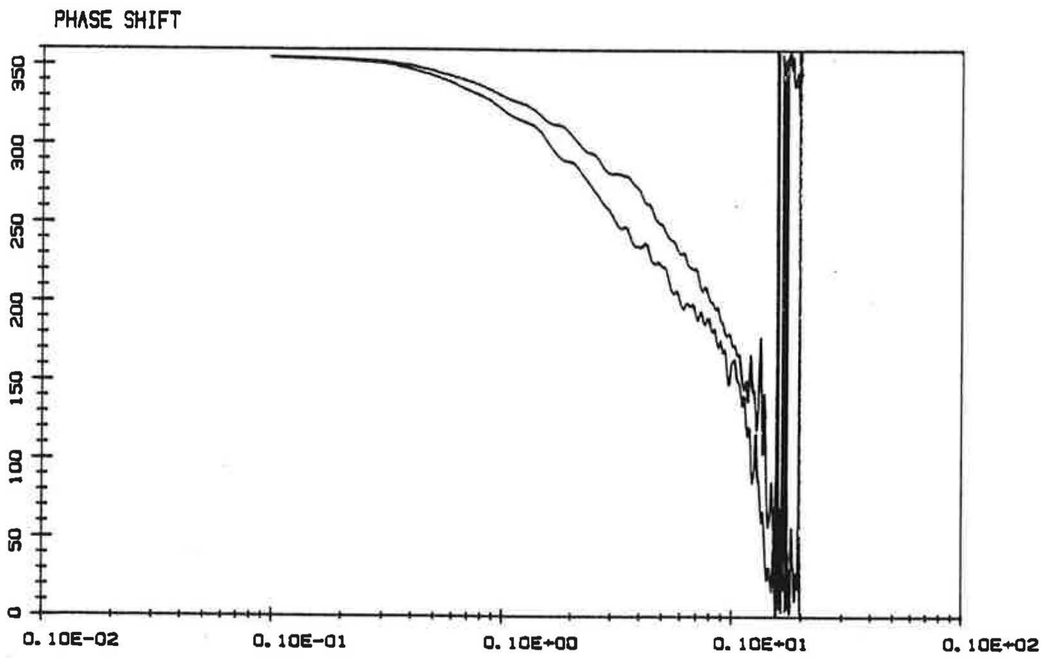

Figure 3.5 Phase shifts corresponding to the transfer functions in Figure 3.3

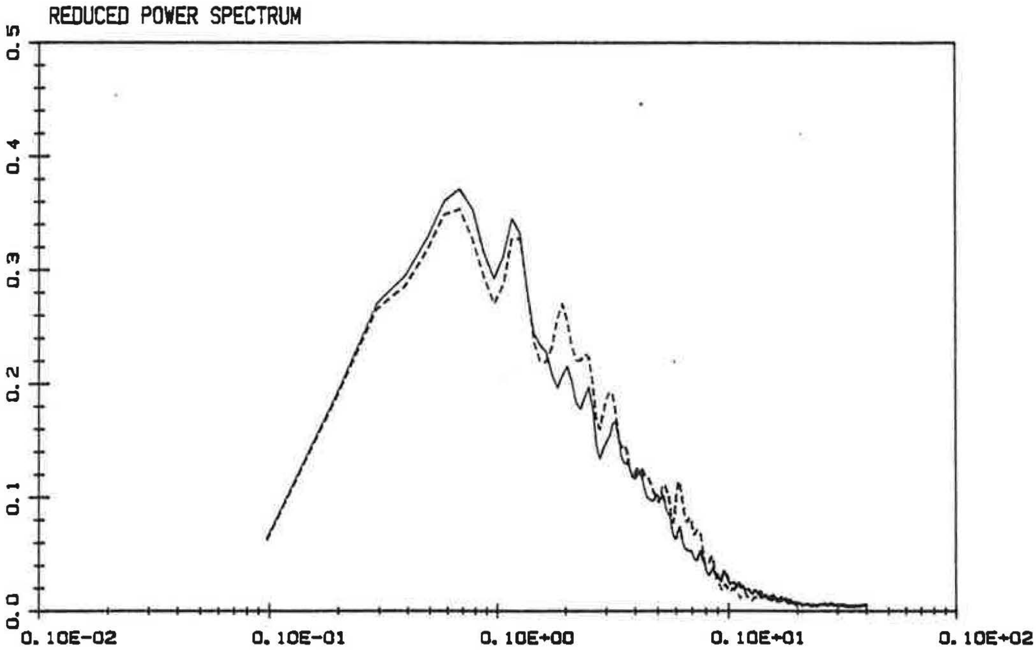

Figure 3.6 Normalized spectra for measurement point No 11.

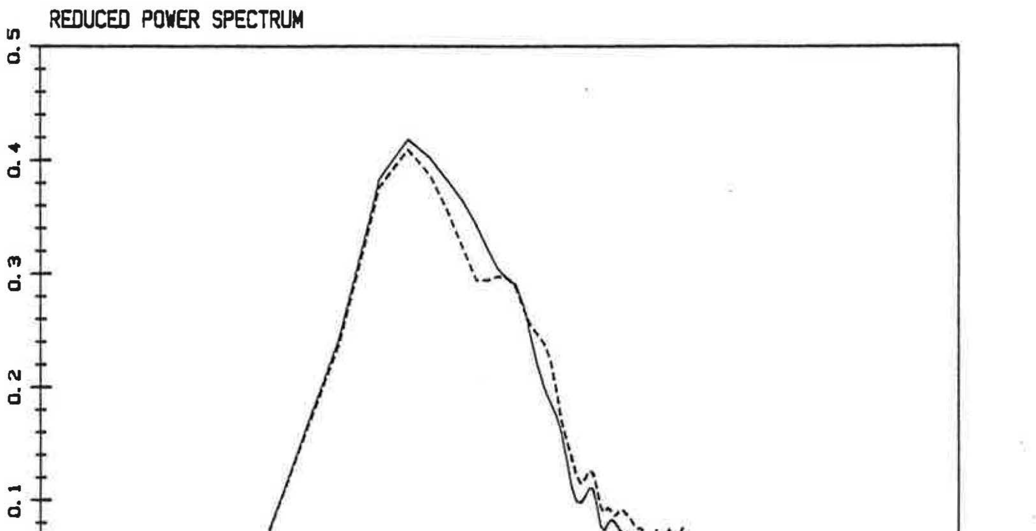

Figure 3.7 Normalized spectra for measurement point No 12.

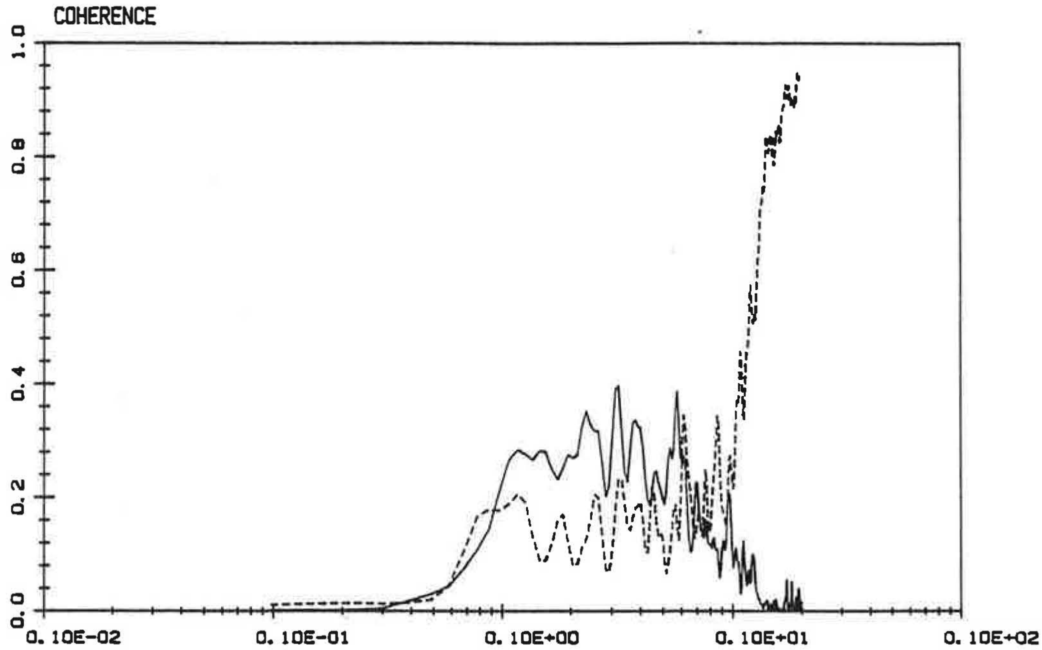

Figure 3.8 Coherence function.

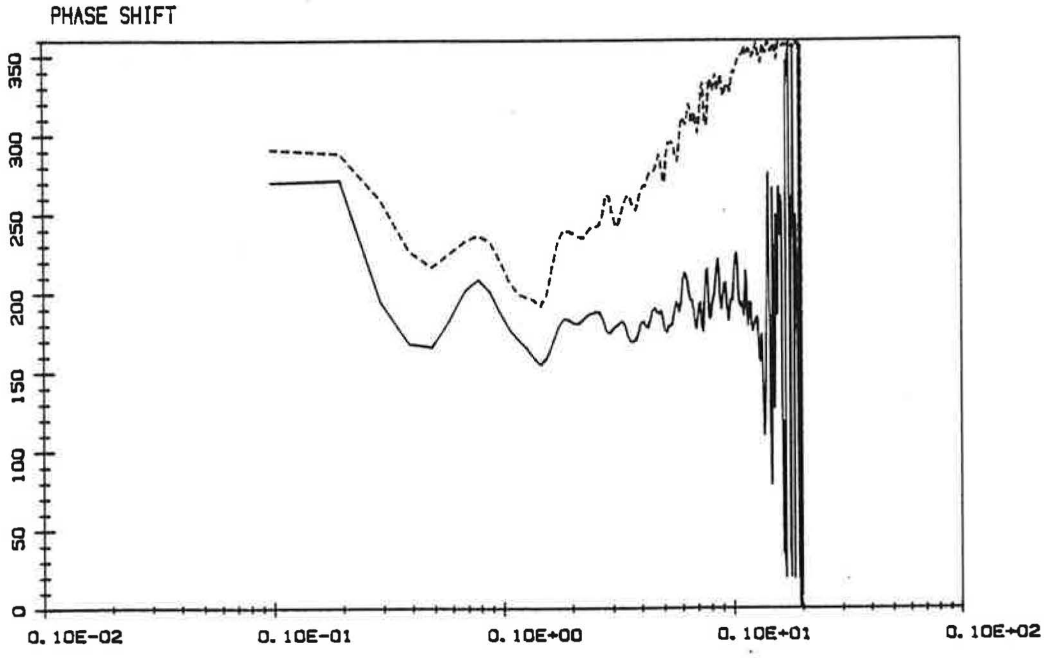

Figure 3.9 Phase shift

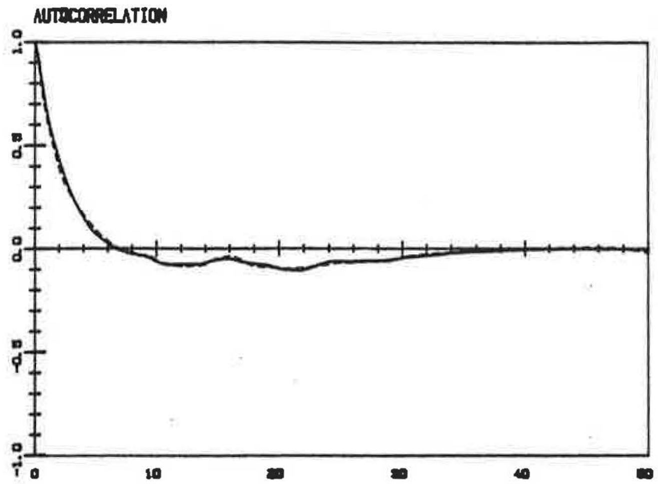

Figure 3.10 Auto-correlation, measurement point No 11.

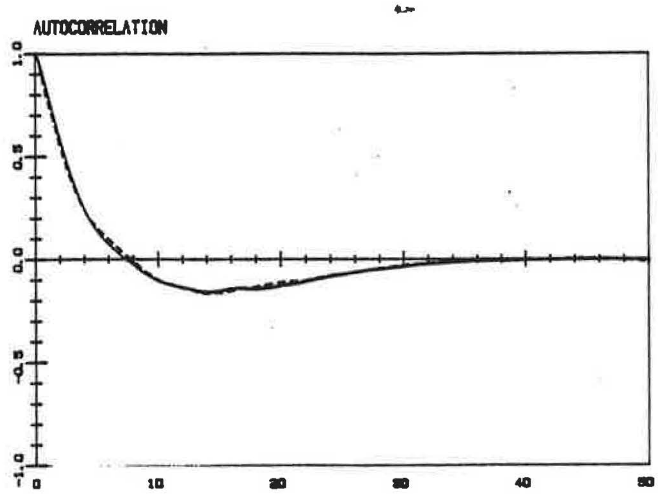

Figure 3.11 Auto-correlation, measurement point No 12.

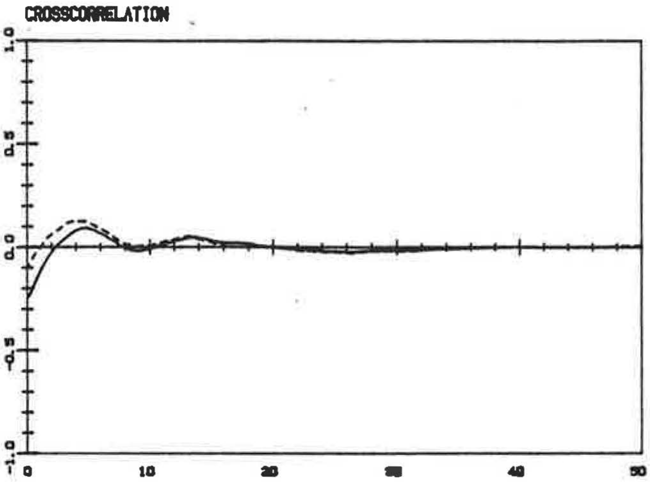

Figure 3.12 Cross-correlation, measurement point No 11

4 REFERENCES

Bendat, J.S. & Piersol, A.G. (1971), *Random data - Analysis and measurement procedures*, Wiley Interscience, New York.

Bergh, H. & Tijdeman, H. (1965), *Theoretical and experimental results for the dynamic response of pressure measuring systems*, NLR-TR F.238. National Aeronautical and Astronautical Research Institute, Amsterdam.

Handa, K. (1985), *Computer program DACSA*, Chalmers University of Technology, Division of Structural Design, unpublished manuscript, Göteborg.

Irwin, H.P.A.H., Cooper, K.R. & Girard, R. (1979), *Correction of distortion effects caused by tubing systems in measurements of fluctuating pressures*, Journal of Industrial Aerodynamics, 5(1979), Amsterdam.

Magnusson, B. (1986), *FFT on the MINC*, Chalmers University of Technology, Division of Structural Design, Report 1986:11, Göteborg.

Robson, J.D. (1963), *An introduction to random vibration*, Edinburgh University Press, Edinburgh.